Neutral-current effects in elastic charged-lepton–nucleon scattering*

D. Cuthiell and John N. Ng
Theoretical Physics Institute, University of Alberta, Edmonton, Alberta, T6G 2J1 Canada
(Received 20 June 1977)

The possibility of observing weak-neutral-current effects in the elastic scattering of charged leptons from nucleons is discussed. General features of different possible polarization experiments (including the possibility of testing for second-class neutral currents) are considered. Polarization asymmetries are calculated for polarized-(lepton)-beam and polarized-target experiments under a wide range of kinematic conditions and for several different gauge models. The desirability of doing these experiments at moderate, rather than very large, momentum transfers is emphasized.

I. INTRODUCTION

The experimental discovery[1] of weak neutral currents (NC's) has provided the motivation for renewed interest in the structure of the weak interactions. Although the existence of neutral currents is commonly regarded as a triumph for unified gauge theories of the weak and electromagnetic interactions, it is also of great interest from a purely phenomenological point of view. In this view, one would like to have an understanding of the neutral current comparable to that provided by the V-A theory of the charged weak current.

So far, almost all our knowledge of neutral currents has come from the scattering of muon neutrinos (ν_μ) on nucleons (N).[1a,1b] Theoretical analyses[2] of these experiments provide a reasonably consistent picture of the neutrino NC as a vector (V) and axial-vector (A) combination.[3] Results are in agreement with the Weinberg-Salam (WS) model[4,5] (although some other unified gauge models are not yet ruled out).

In contrast to the emerging picture of the neutrino NC, there is presently little knowledge of the possible NC interactions of the charged leptons, the electron and muon. Although most gauge models predict neutral currents for the electron and muon, experimental information is still scarce. We have only the (initially contradictory) results of two ν_μ-e elastic scattering experiments,[1c] and the results of two atomic-physics experiments[6] that measure the parity-violating interaction of the outer orbiting electrons with the nucleus of bismuth. Preliminary results of the atomic-physics experiments indicate an effect smaller than that expected from the WS model.[7] It is obviously essential to refine these existing experiments and perform other experiments[8] capable of detecting NC effects for charged leptons.

One difficulty in the search for NC interactions of the charged leptons is that the effects are expected to be of weak-interaction strength while most processes involving charged leptons are dominated by the larger electromagnetic interaction.[9] This necessitates either very-high-precision experiments (such as the atomic-physics experiments) or very-high-energy experiments, since the weak interactions typically grow with energy.

If the NC of the charged leptons is related to the NC detected in ν_μ-hadron scattering, it might be expected to have parity-violating pieces. This suggests studying polarization effects[10,11] as a probe of neutral-current phenomena. Experiments to study such effects have already been initiated by a SLAC-Yale-Bielefeld-Aachen collaboration at SLAC.[12]

The present study is concerned with parity-violating effects in the elastic scattering of charged leptons on nucleons. We consider experiments with the beam, the target, or both the beam and the target polarized. Our assumptions are somewhat less restrictive and our results are more extensive than those of earlier works on this subject.[11]

The process of interest is depicted in Fig. 1, with the NC interaction represented effectively by the exchange of a neutral vector boson, Z [Fig. 1(b)].[13] We will be interested in the interference between the NC graph, Fig. 1(b), and the quantum-electrodynamics contribution, Fig. 1(a). This will contain the effects of any parity-violating piece in either the lepton-Z or nucleon-Z couplings. Two-photon contributions can be ignored since they are parity-conserving and therefore merely provide a small correction to Fig. 1(a).

One appropriate quantity for study is the asymmetry R_B defined by

$$R_B \equiv \frac{(d\sigma/d\Omega)_r - (d\sigma/d\Omega)_l}{(d\sigma/d\Omega)_r + (d\sigma/d\Omega)_l} , \tag{1}$$

where the subscripts r and l denote right- and left-handed helicities of an initially polarized lepton scattering from an unpolarized target. An asymmetry R_T can be similarly defined for a

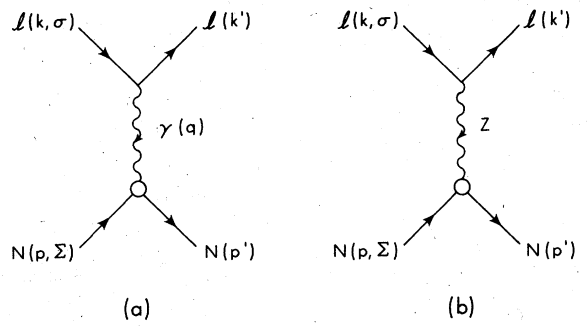

FIG. 1. Effective lowest-order Feynman diagrams for the elastic scattering of a charged lepton from a nucleon with (a) denoting one photon exchange and (b) the exchange of a Z boson.

polarized target and unpolarized beam.

The size of an asymmetry (either polarized target or polarized beam) is, in general, controlled by the NC couplings and by the size of the momentum transfer squared, Q^2 (where $Q^2 \equiv -q^2$, and $q \equiv k - k'$. See Fig. 1.). Thus, the asymmetry has the typical form

$$R = \frac{G_F}{4\pi\sqrt{2}\alpha} Q^2 \mathcal{F} = 7.9 \times 10^{-5} \left(\frac{Q^2}{M^2}\right) \mathcal{F}, \tag{2}$$

with G_F the usual Fermi coupling constant, α the fine-structure constant, M the nucleon mass, and $\mathcal{F}$ a function of the weak and electromagnetic form factors which depends crucially on the assumed form of the neutral-current interaction. For the models we consider, $\mathcal{F}$ is generally of order unity (see Sec. III); although, in special cases (e.g., certain Weinberg angles in the WS model), it can be much smaller. The Q^2 dependence in (2) arises because the denominator in Eq. (1) is essentially given by quantum electrodynamics [i.e., the dominant contribution comes from Fig. 1(a)] and therefore behaves as $1/(Q^2)^2$, whereas the numerator is predominantly an interference between Figs. 1(a) and 1(b) and therefore behaves as $1/Q^2$ for Q^2 small compared to the Z-boson mass squared.

As a test for a parity-violating NC for charged leptons, the polarized elastic scattering experiments we are discussing have the merit of relatively few theoretical uncertainties. Model dependence resides primarily in the neutral-current couplings assumed for different theories. The major uncertainty in confronting specific models with experimental data involves the Q^2 dependences of form factors, which are needed to relate experiments at large Q^2 to predictions for $Q^2 = 0$. Even the commonly adopted assumption of "form-factor scaling"[14] for the nucleon's electromagnetic form factors is not really tested at momentum transfers greater than several $(\mathrm{GeV}/c)^2$, and the behavior of the charged-weak-current form factors, which is used to infer the behavior of the corresponding neutral-current form factors, is even less reliably known. These uncertainties must be weighed against the potential enhancement at large Q^2 given by Eq. (2).

In Sec. II, we present our formulation of the problem in the most general terms. Some of the anticipated effects are discussed, including the possibility of testing for second-class currents. In Sec. III, we specialize to several particular models and compare their numerical predictions under a variety of experimental conditions. Section IV contains further discussion of the results and some concluding remarks.

II. GENERAL CONSIDERATIONS

The kinematics for elastic scattering of a polarized, charged lepton l^- (an electron or muon) from a polarized nucleon target N may be summarized by

$$l(k,\sigma) + N(p,\Sigma) \to l(k') + N(p'), \tag{3}$$

where k (k') and p (p') are the four-momenta of the incoming (outgoing) lepton and the target (recoil) nucleon, respectively, and σ, Σ are the corresponding polarization vectors. Apart from some brief remarks, we restrict our attention to the case that final-state polarizations are not measured.

As discussed in the Introduction, we must examine the interference between Figs. 1(a) and 1(b). The NC interaction, represented by the Z-boson exchange of Fig. 1(b), is assumed to be described by an effective Lagrangian of the current × current form,

$$L_{\mathrm{eff}}^{(N)} = \frac{G_F}{\sqrt{2}} (J^{(N)} + j^{(N)})_\mu (J^{(N)} + j^{(N)})^\mu, \tag{4}$$

where $J_\mu^{(N)}$ is the hadronic NC and $j_\mu^{(N)}$ is the leptonic NC. It is further assumed that $J_\mu^{(N)}$ and $j_\mu^{(N)}$ consist only of V and A terms.[2,3] With this assumption, the leptonic NC takes the form

$$j_\mu^{(N)} = C_V(\bar{e}\gamma_\mu e + \bar{\mu}\gamma_\mu \mu) + C_A(\bar{e}\gamma_\mu\gamma_5 e + \bar{\mu}\gamma_\mu\gamma_5\mu) + \cdots, \tag{5}$$

where C_V and C_A are vector and axial-vector couplings which, at present, are free parameters, and e and μ are the electron and muon fields. The neutrino and possible heavy-lepton NC terms are not displayed explicitly in (5).

For the hadronic NC, $J^{(N)}$, we require only the matrix element between nucleon states. Again, assuming a V and A admixture, we have[5,15]

$$\langle p'|J^{(N)\mu}(0)|p\rangle=\frac{1}{(2\pi)^3(2p_0 2p_0')^{1/2}}\,\bar{u}(p')\left(\gamma^\mu g_V^0+\gamma^\mu\gamma_5 g_A^0+i\frac{q^\mu}{2M}g_S^0+\frac{q^\mu}{2M}\gamma_5 g_P^0+i\frac{q_\lambda}{2M}\sigma^{\mu\lambda}g_T^0+\frac{q_\lambda}{2M}\sigma^{\mu\lambda}\gamma_5 g_{II}^0\right)u(p), \tag{6}$$

where the NC form factors $g_V^0,\ldots,g_{II}^0$ defined by this equation are all real since $J^{(N)\mu}$ is Hermitian. For nucleon targets, the form factors are, in general, a mixture of isovector and isoscalar parts; in practice, we will treat them just as numbers, having different values for a proton or neutron target.

The terms g_S^0 and g_{II}^0 are not present if one assumes that $J_\mu^{(N)}$ is a pure first-class current.[16] Also the g_S^0 term is absent if $J_\mu^{(N)}$ is conserved (as is the case, for example, in the WS model,[5] in which the neutral current is a linear combination of the conserved electromagnetic current and the isotopic partner of the charged weak current, and the vector part of the latter is conserved by the conserved-vector-current hypothesis). However, present experimental evidence does not allow us to exclude these second-class terms.

We also require the matrix element of the electromagnetic current, J_{em}^μ, between nucleon states, written conventionally in the form

$$\langle p'|J_{em}^\mu(0)|p\rangle=\frac{1}{(2\pi)^3(2p_0' 2p_0)^{1/2}}\,\bar{u}(p')\left[\gamma^\mu F_1(Q^2)+\frac{i\kappa\sigma^{\mu\nu}}{2M}q_\nu F_2(Q^2)\right]u(p), \tag{7a}$$

where, for the proton,

$$\kappa^p=1.79,\quad F_1^p(0)=F_2^p(0)=1, \tag{7b}$$

and, for the neutron,

$$\kappa^n=-1.91,\quad F_1^n(0)=0,\quad F_2^n(0)=1. \tag{7c}$$

We shall also be using the Sachs form factors[17] defined by

$$G_M\equiv F_1+\kappa F_2, \tag{8a}$$

$$G_E\equiv F_1-\frac{Q^2}{4M^2}\kappa F_2. \tag{8b}$$

With the above definitions, it is straightforward to obtain the invariant amplitude squared, $|\mathfrak{M}|^2$, for the process (3). Explicitly,

$$|\mathfrak{M}|^2=4\frac{e^4M^4}{(Q^2)^2}T_0+4\frac{G_F e^2M^4}{\sqrt{2}\,Q^2}T_{\gamma Z}+O(G_F^2), \tag{9a}$$

where T_0, the quantum-electrodynamics contribution, is

$$T_0=\left\{\frac{1}{2}\left(\frac{Q^2}{M^2}\right)^2 G_M^2+\frac{G_E^2+G_M^2Q^2/4M^2}{1+Q^2/4M^2}\left[\left(\frac{s}{M^2}-1\right)^2-\frac{Q^2}{M^2}\frac{s}{M^2}\right]\right\}+(\text{polarization-dependent terms}), \tag{9b}$$

and $T_{\gamma Z}$, the interference term, has the form

$$T_{\gamma Z}=r_0+\frac{\Sigma\cdot q}{M}r_1+\frac{\Sigma\cdot k}{M}r_2+\frac{\epsilon_{\mu\nu\rho\lambda}p^\mu\Sigma^\nu q^\rho k^\lambda}{M^3}r_3+m_l\frac{\sigma\cdot p}{M^2}r_4+m_l\frac{\sigma\cdot q}{M^2}r_5+\frac{m_l}{M^3}(\sigma\cdot q)(\Sigma\cdot q)r_6$$
$$+\frac{m_l}{M^3}(\sigma\cdot q)(\Sigma\cdot k)r_7+\frac{m_l}{M^3}(\sigma\cdot p)(\Sigma\cdot q)r_8+\frac{m_l}{M}\sigma\cdot\Sigma r_9+\frac{m_l}{M^3}\epsilon_{\mu\nu\rho\lambda}p^\mu\sigma^\nu q^\rho\Sigma^\lambda r_{10}+\frac{m_l}{M^2}(\sigma\cdot q)\frac{\epsilon_{\mu\nu\rho\lambda}p^\mu k^\nu q^\rho\Sigma^\lambda}{M^3}r_{11}. \tag{9c}$$

Here, s is the usual Mandelstam variable, $s=(k+p)^2$, and m_l is the lepton mass.

The "polarization-dependent terms" of Eq. (9b) have the same dependences on σ and Σ as the r_6, r_8, and r_9 terms in (9c). They will not be given explicitly here.

The term r_0 in Eq. (9c), which is independent of σ and Σ, effectively supplies only a weak correction to T_0 and will therefore be neglected in our numerical calculations. The remaining dimensionless factors r_i $(i=1,2,\ldots,11)$ are given by

$$r_1=\frac{1}{M^2}\left\{G_M[-2C_V g_A^0(s-M^2-Q^2)-2C_A(g_V^0+g_T^0)Q^2]+\kappa F_2 C_V g_A^0(s-M^2-\tfrac{1}{2}Q^2)\left(1+\frac{s}{M^2}\right)\right.$$
$$\left.+\tfrac{1}{2}C_A[G_M g_T^0+\kappa F_2(g_V^0+g_T^0)]Q^2\left(1+\frac{s}{M^2}\right)\right\}, \tag{10a}$$

$$r_2=\frac{2}{M^2}\{G_M[C_V g_A^0(2s-2M^2-Q^2)+2C_A(g_V^0+g_T^0)Q^2]-\kappa F_2 C_V g_A^0(2s-2M^2-Q^2)(1+Q^2/4M^2)$$
$$-C_A[G_M g_T^0+\kappa F_2(g_V^0+g_T^0)]Q^2(1+Q^2/4M^2)\}, \tag{10b}$$

$$r_3=G_M C_A g_\Pi^0\cdot Q^2/M^2, \tag{10c}$$

$$r_4=\frac{2}{M^2}\left[2G_M C_V g_A^0 Q^2+C_A\left(F_1 g_V^0+\kappa F_2\, g_T^0\frac{Q^2}{4M^2}\right)(2s-2M^2-Q^2)\right], \tag{10d}$$

$$r_5=\frac{2}{M^2}\left\{G_M[C_V g_A^0 Q^2-C_A(g_V^0+g_T^0)Q^2]+C_A\left(F_1 g_V^0+\kappa F_2 g_T^0\frac{Q^2}{4M^2}\right)(s+M^2)\right\}, \tag{10e}$$

$$r_6=G_M[-4C_A g_A^0+C_A g_P^0(s/M^2-1)+4C_V g_V^0+2C_V g_T^0]+\kappa F_2[2C_A g_A^0-C_A g_P^0(s/M^2-1)-2C_V(g_V^0+g_T^0)], \tag{10f}$$

$$r_7=G_M(4C_A g_A^0-C_A g_P^0 Q^2/M^2), \tag{10g}$$

$$r_8=G_M\left[-4C_A g_A^0+C_A g_P^0\frac{Q^2}{M^2}+C_V g_T^0\frac{Q^2}{M^2}\right]+\frac{\kappa F_2}{M^2}[C_A g_A^0(2s+2M^2-Q^2)-C_A g_P^0 Q^2+C_V(g_V^0+g_T^0)Q^2], \tag{10h}$$

$$r_9=\frac{1}{M^2}\left\{G_M\left[4C_A g_A^0(s-M^2)-\tfrac{1}{2}C_A g_P^0\frac{(Q^2)^2}{M^2}+4C_V(g_V^0+g_T^0)Q^2-2C_V g_V^0 Q^2\left(1+\frac{Q^2}{4M^2}\right)\right]\right.$$
$$\left.+2\kappa F_2\left[-C_A g_A^0\left(1+\frac{Q^2}{4M^2}\right)(2s-2M^2-Q^2)-C_V(g_V^0+g_T^0)Q^2\left(1+\frac{Q^2}{4M^2}\right)\right]\right\}, \tag{10i}$$

$$r_{10}=-G_M(C_V g_\Pi^0-C_A g_S^0)Q^2/M^2, \tag{10j}$$

$$r_{11}=2G_M C_A g_S^0. \tag{10k}$$

In the remainder of the paper, we will implicitly be considering either electrons of energy greater than 400 MeV or muons of energy greater than 100 GeV. With this assumption, it is a very good approximation to neglect lepton masses relative to lepton energies, which has been done in Eq. (10).

For the sake of completeness, we note that if both the target and incoming beam are unpolarized and one wishes to measure the outgoing lepton polarization, σ', one can use equations similar to (9) and (10) (with $\Sigma=0$) by making the replacements

$$r_4\frac{\sigma\cdot p}{M^2}\to\frac{\sigma'\cdot p}{M^4}\left[2G_M C_V g_A^0 Q^2+C_A\left(F_1 g_V^0+\kappa F_2 g_T^0\frac{Q^2}{4M^2}\right)(2s-2M^2-Q^2)\right] \tag{11a}$$

and

$$r_2\frac{\sigma\cdot q}{M^2}\to\frac{\sigma'\cdot q}{M^4}\left[G_M C_V g_A^0 Q^2+C_A\left(F_1 g_V^0+\kappa F_2 g_T^0\frac{Q^2}{4M^2}\right)(s-3M^2-Q^2)+G_M C_A(g_V^0+g_T^0)Q^2\right]. \tag{11b}$$

We wish now to consider some general features of three possible types of experiments, characterized by the following: (a) polarized lepton beam and unpolarized target, (b) unpolarized beam, polarized target, and (c) polarized beam, polarized target. In the discussion of Sec. I, we emphasized that theoretical predictions become increasingly uncertain for large momentum transfers due to a lack of concrete knowledge of form-factor behaviors. There is another, more practical reason for avoiding high Q^2. Briefly, although asymmetries like R_B [Eq. (1)] are expected to increase with Q^2, the differential cross sections which must be measured are falling so quickly, due to both propagator and form-factor effects, that statistical uncertainties may actually be greater[18] for large Q^2. (These remarks will be amplified in Sec. IV.) Accordingly, in the remainder of this section, we will be particularly interested in results which may be expected at relatively small Q^2. In Sec. III, predictions will be made for larger Q^2 as well, at the expense of additional assumptions.

A. Polarized lepton, unpolarized nucleon

The quantity of interest here is the asymmetry R_B defined by Eq. (1). To calculate R_B, we keep only the contributions of order α^2 in the denominator of (1); that is, only T_0 from Eq. (9a). For an unpolarized target, only the r_4 and r_5 terms from (9c) contribute to the numerator of (1). Explicitly,

$$R_B=\frac{G_F M^2}{4\pi\alpha\sqrt{2}}\,\frac{Q^2}{M^2}\,\frac{1}{T_0}\left(\frac{m_l\sigma_r\cdot p}{M^2}r_4+\frac{m_l\sigma_r\cdot q}{M^2}r_5\right)$$
$$=7.91\times10^{-5}\frac{Q^2}{M^2}\,\frac{1}{T_0}\left(\frac{m_l\sigma_r\cdot p}{M^2}r_4+\frac{m_l\sigma_r\cdot q}{M^2}r_5\right), \tag{12}$$

where r_4, r_5 are given by Eqs. (10d), (10e), respectively, and σ_r is a right-handed polarization vector. Hence, R_B depends in a fairly complicated way upon the three combinations of form factors $C_V g_A^0$, $C_A g_V^0$, and $C_A g_T^0$. However, in certain kinematic regions, the expression (12) simplifies somewhat. In particular, from the expressions

$$m_l \sigma_r \cdot p = \tfrac{1}{2}(s - M^2), \tag{13a}$$

$$m_l \sigma_r \cdot q = -\tfrac{1}{2}Q^2, \tag{13b}$$

it is seen that the r_4 term will dominate (12) when $Q^2 \ll s - M^2$. For a proton target, this kinematic condition produces a further simplification; the C_A terms in r_4 dominate[19] over the C_V term. Consequently, R_B (proton) takes the approximate form

$$R_B(\text{proton}) \simeq 1.6 \times 10^{-4}\left(\frac{Q^2}{M^2}\right)\frac{1 + Q^2/4M^2}{(G_E^p)^2 + (G_M^p)^2 Q^2/4M^2} \times C_A(F_1^p g_V^{0,p} + \kappa^p F_2^p g_T^{0,p} Q^2/4M^2) \tag{14}$$

for $Q^2 \ll s - M^2$. (The superscripts p indicate proton values.) The electromagnetic form factors are known experimentally, at least for moderate Q^2 (see Sec. III); thus, the only unknown quantities in (14) are $C_A g_V^{0,p}$ and $C_A g_T^{0,p}$. Unless the Q^2 dependences of $g_V^{0,p}$ and $g_T^{0,p}$ are assumed, these two quantities cannot, in general, be separately extracted from the combination

$$C_A(F_1^p g_V^{0,p} + \kappa^p F_2^p g_T^{0,p} Q^2/4M^2)$$

except for Q^2 sufficiently small that the $g_V^{0,p}$ term dominates the combination. In the latter case ($Q^2 \ll 4M^2$), it is reasonable to replace all form factors by their values at $Q^2 = 0$, and a very simple result is obtained:

$$R_B(\text{proton}) \simeq 1.6 \times 10^{-4}\left(\frac{Q^2}{M^2}\right) C_A g_V^{0,p}(0), \quad \text{for } Q^2 \ll 4M^2. \tag{15}$$

Therefore, in principle, one can isolate the combination of form factors $C_A g_V^{0,p}$ at very small Q^2.

For a neutron target, the above discussion must be slightly modified. Although the r_4 term still dominates (12) for $Q^2 \ll s - M^2$, an equation like (14) holds only under slightly more stringent conditions. The reason is that $F_1^n(0) = 0$, and therefore the C_V term in r_4 can be as large as the C_A term for a neutron. The only region in which the C_A terms should dominate is $s \gg 4M^2$ (assuming the g_V^0 and g_T^0 terms are of comparable magnitude, which will be true, for example, under the assumptions of Sec. III). Then

$$R_B(\text{neutron}) \simeq 1.6 \times 10^{-4}\left(\frac{Q^2}{M^2}\right)\frac{1 + Q^2/4M^2}{(G_E^n)^2 + (G_M^n)^2 Q^2/4M^2} \times C_A(F_1^n g_V^{0,n} + \kappa^n F_2^n g_T^{0,n} Q^2/4M^2), \tag{16}$$

under the conditions $Q^2 \ll s - M^2$ and $4M^2 \ll s$.

The foregoing arguments and the results (14), (15), and (16) have assumed implicitly that $C_A \neq 0$. However, if it can be established by independent means that $C_A = 0$, the results are quite different. In this case, only the combination $C_V g_A^0$ is represented in R_B. Again assuming $Q^2 \ll s - M^2$,

$$R_B \simeq 1.6 \times 10^{-4}\left(\frac{Q^2}{M^2}\right)\left(\frac{Q^2}{s - M^2}\right) \times \frac{1 + Q^2/4M^2}{G_E^{\,2} + Q^2/4M^2 G_M^{\,2}} G_M C_V g_A^0 \tag{17}$$

for $C_A = 0$. This result holds for either a proton or neutron target with the appropriate choice of form factors.

The form of (17) suggests a simple test (for $C_A = 0$) of the isospin character of g_A^0. We define the ratio

$$E_B \equiv \frac{[(d\sigma/d\Omega)_r - (d\sigma/d\Omega)_l]^p}{[(d\sigma/d\Omega)_r - (d\sigma/d\Omega)_l]^n}, \tag{18}$$

where p and n indicate proton and neutron cross sections. Then if g_A^0 is a purely isovector quantity (as is the case for the models to be discussed in Sec. III), $g_A^{0,p} = -g_A^{0,n}$, and E_B becomes just

$$E_B \simeq -\frac{G_M^p}{G_M^n}, \quad \text{for } Q^2 \ll s - M^2 \quad (C_A = 0). \tag{19}$$

Thus, if $C_A = 0$, a deviation from (19) would signify an isoscalar piece in g_A^0. (For $C_A \neq 0$, it will be more difficult to test the isospin structure of form factors.)

Having discussed several special cases, we wish to consider briefly a more general question: for a given Q^2, how can one separately determine $C_V g_A^0$, $C_A g_V^0$, and $C_A g_T^0$? Evidently one must first choose a range of energy such that s and Q^2 are of comparable magnitude so that all three form factors are represented significantly in R_B. Then, in principle, one can separate the form factors by utilizing the different s dependences of the terms in (12); that is, one must obtain experimental results for Q^2 fixed and different values of total energy.

B. Unpolarized lepton, polarized nucleon

For an arbitrary target polarization, the terms r_1, r_2, and r_3 of Eq. (9c) all contribute to the scattering cross section. However, in the particular case of a target polarized in the direction of the lepton beam, only r_1 and r_2 contribute to the asymmetry defined by

$$R_T^l \equiv \frac{(d\sigma/d\Omega)_\uparrow - (d\sigma/d\Omega)_\downarrow}{(d\sigma/d\Omega)_\uparrow + (d\sigma/d\Omega)_\downarrow}, \tag{20}$$

where $(d\sigma/d\Omega)_\uparrow$ and $(d\sigma/d\Omega)_\downarrow$ are the differential

cross sections for target polarizations parallel and antiparallel, respectively, to the beam direction. R_T^l takes the explicit form

$$R_T^l = \frac{G_F M^2}{4\pi\alpha\sqrt{2}} \frac{Q^2}{M^2} \frac{1}{T_0} \left(\frac{\Sigma_\uparrow \cdot q}{M} r_1 + \frac{\Sigma_\uparrow \cdot k}{M} r_2 \right)$$
$$= 7.91 \times 10^{-5} \frac{Q^2}{M^2} \frac{1}{T_0} \left(\frac{\Sigma_\uparrow \cdot q}{M} r_1 + \frac{\Sigma_\uparrow \cdot k}{M} r_2 \right) \quad (21)$$

where T_0, r_1, and r_2 are given by Eqs. (9b), (10a), and (10b), respectively, and $\Sigma_\uparrow$ is a polarization parallel to the beam. Like R_B discussed previously, R_T^l depends, in general, upon the three combinations of form factors $C_V g_A^0$, $C_A g_V^0$, and $C_A g_T^0$. However, in the kinematic range $Q^2 \ll s - M^2$, the $C_V g_A^0$ terms are dominant and R_T^l assumes the form

$$R_T^l \simeq -1.6 \times 10^{-4} \frac{Q^2}{M^2} C_V g_A^0 \frac{1}{T_0} f_T(Q^2, s), \quad (22a)$$

where the factor $f_T(Q^2, s)$, like T_0, depends only on the known electromagnetic form factors of the target and the variables Q^2, s,

$$f_T(Q^2, s) = \left[\kappa F_2 \frac{Q^2}{4M^2} \left(1 + \frac{s}{M^2} \right)^2 + G_E \left(\frac{s}{M^2} - 1 \right)^2 \right]. \quad (22b)$$

The simple form of (22a) again suggests a possible test for the isospin character of g_A^0. Proceeding in analogy with Sec. IIA, we define

$$E_T \equiv \frac{[(d\sigma/d\Omega)_\uparrow - (d\sigma/d\Omega)_\downarrow]^p}{[(d\sigma/d\Omega)_\uparrow - (d\sigma/d\Omega)_\downarrow]^n}. \quad (23)$$

Then, if g_A^0 is a pure isovector (i.e., $g_A^{0,p} = -g_A^{0,n}$),

$$E_T \simeq -\frac{f_T^p(Q^2, s)}{f_T^n(Q^2, s)}, \quad \text{for } Q^2 \ll s - M^2. \quad (24)$$

We turn now to the intersting case of a target polarized perpendicular to the beam direction. Here, only r_1 and r_3 come into play. The r_3 term has the form, in the laboratory coordinate system,

$$-\frac{\vec{q} \cdot \vec{\Sigma} \times \vec{k}}{M^2} G_M C_A g_\Pi^0 \frac{Q^2}{M^2}. \quad (25)$$

Since the r_1 term has different spin dependence, $\Sigma \cdot q$, it is possible, with the appropriate experimental geometry—namely, $\vec{\Sigma}$ perpendicular to the scattering plane—to isolate the r_3 term. If C_A were established to be nonzero, a polarization effect with this geometry would clearly signify the existence of second-class neutral currents.

In summary, polarized-target experiments, while more difficult,[20] offer the hope of directly measuring a different combination of form factors from that which is measured in polarized-beam experiments [compare Eqs. (14), (22)]. They may also provide a test for second-class neutral currents.

C. Polarized lepton, polarized nucleon

We have seen that by using a polarized target and unpolarized beam, one can, in principle, measure the hadronic NC form factors g_V^0, g_T^0, g_A^0, and g_Π^0. However, such experiments are not sensitive to the form factors g_P^0 and g_S^0. To measure the latter, experiments must ultimately be done with both polarized beam and polarized target.

In addition to the formidable problems of even doing such experiments, there are difficulties with extracting the desired information. In particular, the terms r_6, r_8, and r_9 are completely dominated by QED contributions with the same polarization dependences [see Eq. (9b)]. Hence, to isolate, say, g_P^0 would require measuring the term r_7, that is, separating the polarization correlations characteristic of the r_7 term from the much larger QED correlations. The detection of the second-class form factor g_S^0 is equally difficult; one must separate out the correlations of r_{10} and/or r_{11}, which have the forms in the laboratory frame

$$\vec{q} \cdot \vec{\Sigma} \times \vec{\sigma}$$

and

$$(\sigma \cdot q) \left(\frac{\vec{k} \cdot \vec{q} \times \vec{\Sigma}}{M^2} \right),$$

respectively. We should note that the above two correlations are sensitive only to second-class terms, g_S^0 or g_Π^0. Furthermore, if C_A were zero, a nonzero g_Π^0 would contribute only through r_{10} (no longer r_3), and no experiment could measure g_S^0.

III. MODELS AND NUMERICAL CALCULATIONS

Many gauge models make definite predictions for the values of the NC form factors and consequently for the asymmetries R_T and R_B discussed in Sec. II. To obtain the numerical results described in this section, we have considered the WS model, the E_7 model,[21] and several phenomenological models in which the leptonic NC is either pure V, pure A, or $V-A$. The phenomenological models are studied not from any theoretical motivation but because they illustrate the dependence of the effects on C_V and C_A.

The purely vectorlike gauge models discussed by several authors[22] give no parity-violating asymmetries and furthermore, appear to disagree[2] with existing $\nu_\mu N$ scattering data. Hence, the models are not considered here.

The quantities which must be extracted from the

gauge models are C_V, C_A, and the hadronic form factors $g_V^0, g_T^0, \ldots$ [see Eq. (6)]. All existing gauge theories assume that the two second-class terms g_Π^0 and g_S^0 are absent. The remaining hadronic form factors are related to the corresponding charged weak-current form factors and the electromagnetic form factors by simple linear equations (for the models considered here)

$$g_V^0 = \pm\alpha g_V + \beta F_1 , \tag{26a}$$

$$g_T^0 = \pm\gamma g_T + \eta(\kappa F_2) , \tag{26b}$$

$$g_A^0 = \pm\rho g_A , \tag{26c}$$

$$g_P^0 = \pm\tfrac{1}{2} g_P . \tag{26d}$$

The ± signs in (26) refer to proton and neutron targets, respectively. The coefficients $\alpha, \beta, \ldots$ depend on the gauge model considered and are listed, for the models of interest, in Table I. For the WS and E_7 models, these parameters are taken from the work of other authors[5,21]; for the phenomenological models, we simply assume that the neutral form factors are obtained from the charged form factors by an isospin rotation (thus they are pure isovector). The parameter x_W in Table I denotes $\sin^2\theta_W$, where θ_W is the weak angle of the model. For the WS model, we allow different values of x_W between 0.2 and 0.5, whereas, for the E_7 model, we consider only $x_W = 0.4$, as suggested by the analysis[2] of the $\nu_\mu N$ data. The three different versions of the E_7 model, having different values of C_V and C_A, correspond to different assignments of leptons to representations of the group.

To perform numerical calculations, we require the Q^2 dependence of the electromagnetic form factors and the charged weak form factors g_V, g_T, and g_A [see Eq. (26)]. This is assumed, in all cases to be of the dipole form, which is at least approximately verified at low Q^2 by existing data.[23,24] Specifically, we use

$$G_M^p(Q^2) = \frac{(1+\kappa^p)}{(1+Q^2/M_V^2)^2} , \tag{27a}$$

$$G_E^p(Q^2) = \frac{1}{(1+Q^2/M_V^2)^2} , \tag{27b}$$

$$G_M^n(Q^2) = \frac{\kappa^n}{(1+Q^2/M_V^2)^2} , \tag{27c}$$

$$G_E^n(Q^2) = 0 , \tag{27d}$$

$$g_V(Q^2) = \frac{1}{(1+Q^2/M_V^2)^2} , \tag{27e}$$

$$g_T(Q^2) = \frac{3.70}{(1+Q^2/M_V^2)^2} , \tag{27f}$$

$$g_A(Q^2) = \frac{1.24}{(1+Q^2/M_A^2)^2} . \tag{27g}$$

TABLE I. Neutral-current parameters for different models of interest [see Eq. (26)].

Model	C_V	C_A	α	β	γ	η	ρ
WS	$4x_W-1$	1	$\frac{1}{2}$	$-2x_W$	$\frac{1}{2}$	$-2x_W$	$-\frac{1}{2}$
$V-A$	1	−1	$\frac{1}{2}$	0	$\frac{1}{2}$	0	$-\frac{1}{2}$
V	1	0	$\frac{1}{2}$	0	$\frac{1}{2}$	0	$-\frac{1}{2}$
A	0	1	$\frac{1}{2}$	0	$\frac{1}{2}$	0	$-\frac{1}{2}$
E_7(A)	$-4x_W+3$	1	0	$\frac{3}{2}-2x_W$	0	$\frac{3}{2}-2x_W$	$-\frac{1}{4}$
E_7(B)	$-4x_W+3$	−1	0	$\frac{3}{2}-2x_W$	0	$\frac{3}{2}-2x_W$	$-\frac{1}{4}$
E_7(C)	$4x_W-1$	0	0	$\frac{3}{2}-2x_W$	0	$\frac{3}{2}-2x_W$	$-\frac{1}{4}$

The value of M_V^2 can be taken to be 0.71 GeV^2; however, M_A^2 is not so well known.[24] In most of our calculations (unless otherwise stated) we take $M_A^2 = 0.71$ GeV^2, but in special cases we compare with results assuming $M_A^2 = 1.32$ GeV^2. (Both values are consistent with present data.)

Making the assumptions described above, asymmetries can be calculated for the various models. In the remainder of this section, we will discuss some of these calculations.

Figures 2(a)–2(d) show the behavior of the asymmetry R_B, for a proton target, as a function of the scattering angle θ. The WS model is used, with three possible values, 0.2, 0.4, and 0.5, for the parameter x_W and four different lepton energies, 0.4, 5, 20, and 150 GeV. The graphs illustrate some of our earlier general considerations. The most obvious feature is the expected increase in R_B with Q^2. Thus, for example, although R_B does not exceed 10^{-5} for lepton energy $\omega = 400$ MeV, it can reach the value 10^{-3} for $\omega = 20$ GeV, $\theta = 12^\circ$ if $x_W = 0.5$.

The variation of R_B with x_W can also be partially understood from previous discussions. For very small angles, in particular, Q^2 is small and Eq. (15) is approximately valid; that is, R_B depends on the combination $C_A g_V^{0,p}$. Substituting the form-factor values from Eq. (26a) and Table I into (15) gives the approximate result

$$R_B(\text{proton}) \simeq 8.0\times10^{-5}\left(\frac{Q^2}{M^2}\right)(1-4x_W) . \tag{28}$$

(We have used $g_V(0) = F^p(0) = 1$ in writing this.) A consequence of (28), which is seen in Fig. 2, is that the $x_W = 0.5$ model has the largest asymmetries at small angles. More generally, (28) indicates that in the context of the WS model, a measurement of the slope of R_B(proton) vs Q^2 for small Q^2 would give the value of x_W.

For larger angles, the $x_W = 0.4$ predictions remain smaller, but the $x_W = 0.2$ values can reach a magnitude comparable with those of $x_W = 0.5$.

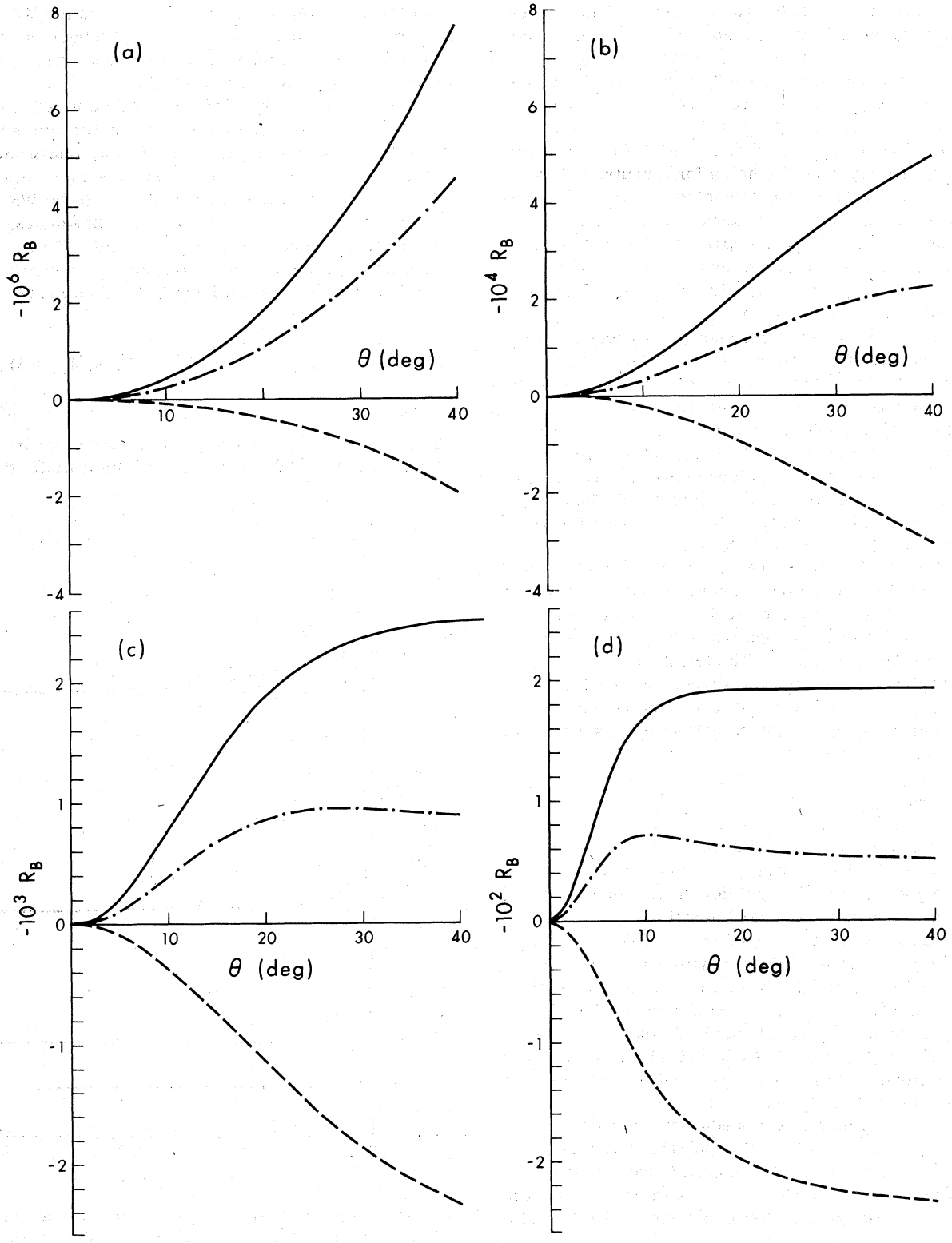

FIG. 2. The asymmetry R_B (see text) as a function of the scattering angle θ for a proton target and lepton energies (a) $\omega = 400$ MeV, (b) $\omega = 5$ GeV, (c) $\omega = 20$ GeV, and (d) $\omega = 150$ GeV, in the WS model. The solid curves are for $x_W = 0.5$, the dash-dot curves are for $x_W = 0.4$, and the dashed curves are for $x_W = 0.2$.

A comparison of the values of R_B for proton and neutron targets can be made from Table II. (The models and kinematic ranges are those of Fig. 2, with the addition of $x_W = 0.33$.) In most cases, the neutron asymmetries are larger in magnitude than the corresponding proton values; however, a notable exception is $x_W = 0.5$, for $\omega \geq 5$ GeV. No equation as simple as (28) holds for a neutron target (see Sec. II A) but the predicted asymmetries show a similarly strong dependence on x_W compared with their proton counterparts.[25] An interesting feature of the neutron values is that, in some cases (e.g., $x_W = 0.5$, $\omega = 20$ GeV) they display a zero in the angular range $0 < \theta < 40°$.

In Fig. 3, we show the energy dependence of R_B for several fixed values of Q^2. These results assume the WS model with $x_W = 0.4$ (henceforth called the standard model). For sufficiently large energies, R_B becomes constant. This occurs because the leading behavior of both T_0 and $T_{\gamma Z}$ in Eq. (9a), and hence both the denominator and numerator of Eq. (1), for large s, is just s^2. The asymptotic values of R_B in Fig. 3 increase linearly with Q^2, in accord with Eq. (2).

The predictions of the different models are compared, for a fixed beam energy of 20 GeV, in Fig. 4. (We have chosen $x_W = 0.4$ in the WS model as our point of comparison since this is the value indicated by $\nu_\mu N$ data.[2]) The two models with $C_A = 0$ give the smallest asymmetries, at least for small angles. This is expected from Eqs. (14) and (17); the latter equation, which holds for $C_A = 0$, has an extra factor of

$$\frac{Q^2}{(s - M^2)}.$$

Asymmetries in the axial-vector model ($C_A = 1$, $C_V = 0$), the V-A model, and two of the E_7 models are considerably larger, for these kinematics, than those in the standard model.

As has been emphasized in Sec. II A, the asymmetry R_B probes the combination $C_A g_V^0$ and thus should be relatively insensitive to the choice of $M_A{}^2$ in Eq. (27g). This is confirmed by Fig. 5, which shows R_B in the standard model for $\omega = 20$ GeV, and the two values $M_A{}^2 = 0.71$ and 1.32 GeV^2. Significant differences appear only for Q^2 greater than around 10 (GeV/c)^2, i.e., $\theta > 10°$.

Next we will discuss predictions of different models for scattering of unpolarized leptons from polarized targets. Our emphasis will be on results for longitudinally polarized targets (i.e., target polarization parallel or antiparallel to the beam direction).

Figures 6(a)–6(d) show the dependence of the longitudinally polarized target asymmetry, R_T^l, on scattering angle for four different lepton energies and three values of the parameter x_W in the WS model. The graphs are for a proton target; a comparison with the corresponding neutron target results may be made from Table III.

As discussed in Sec. II B, R_T^l is dominated, for Q^2 less than $(s - M^2)$, by the form-factor combination $C_V g_A^0$. This is apparent in Fig. 6, where the dependence of the asymmetry on x_W simply reflects the corresponding dependence in C_V. If the WS model is a valid description of these phenomena, accurate measurement of R_T^l for small Q^2 will provide the value of the parameter x_W. Substituting Eq. (26c) and values from Table I into (22a), we have explicitly

$$R_T^l(\text{proton}) \simeq 8.0 \times 10^{-5} \left(\frac{Q^2}{M^2}\right) \frac{1}{T_0} f_T(Q^2, s)(4x_W - 1), \tag{29}$$

for $Q^2 \ll (s - M^2)$, where f_T and T_0 are given by Eqs. (22b) and (9b), respectively. Essentially the

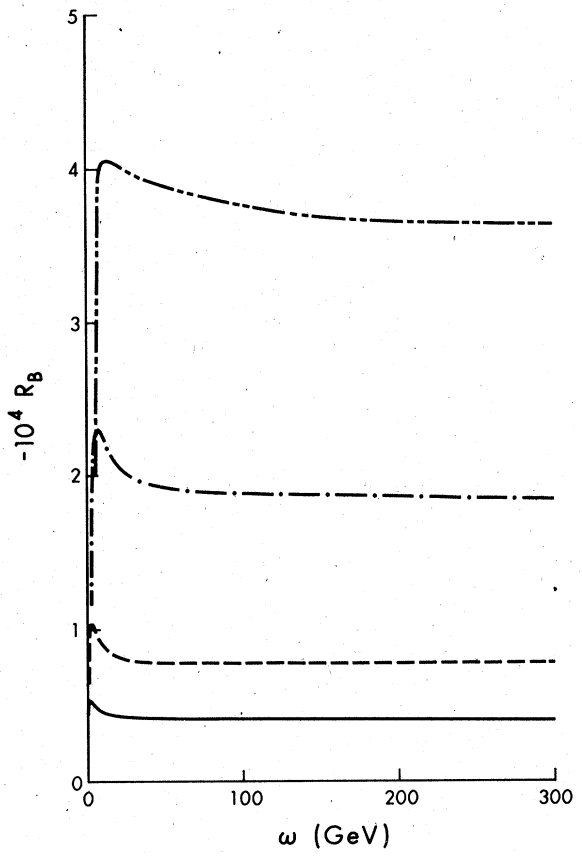

FIG. 3. The asymmetry R_B (proton target) as a function of incoming energy ω for different fixed Q^2 in the standard model (i.e., WS model with $x_W = 0.4$). The solid curve is for $Q^2 = 1$ (GeV/c)^2, the dashed curve is for $Q^2 = 2$ (GeV/c)^2, the dash-dot curve is for $Q^2 = 5$ (GeV/c)^2, and the dash-double-dot curve is for $Q^2 = 10$ (GeV/c)^2.

TABLE II. Values of the asymmetry R_B [see Eq. (1)] for the standard gauge model. (The upper number for each scattering angle θ is for a proton target and the number in parentheses is for a neutron target.)

Q^2 [(GeV/c)^2]	θ \ x_W	0.2	0.33	0.4	0.5
		(a) $\omega = 400$ MeV			
4.87×10^{-5}	1°	8.77×10^{-10}	-1.40×10^{-9}	-2.63×10^{-9}	-4.38×10^{-9}
		(9.94×10^{-9})	(7.29×10^{-10})	(-4.23×10^{-9})	(-1.13×10^{-8})
7.79×10^{-4}	4°	1.41×10^{-8}	$-2.25 \times 10^{-8})$	-4.21×10^{-8}	$-7.02 \times 10^{-8})$
		(1.59×10^{-7})	(1.17×10^{-8})	(-6.76×10^{-8})	(-1.81×10^{-7})
4.83×10^{-3}	10°	8.98×10^{-8}	-1.41×10^{-7}	-2.65×10^{-7}	-4.43×10^{-7}
		(9.85×10^{-7})	(7.35×10^{-8})	(-4.17×10^{-7})	(-1.12×10^{-6})
4.06×10^{-2}	30°	9.59×10^{-7}	-1.30×10^{-6}	-2.51×10^{-6}	-4.24×10^{-6}
		(8.22×10^{-6})	(7.00×10^{-7})	(-3.35×10^{-6})	(-9.13×10^{-6})
6.81×10^{-2}	40°	1.92×10^{-6}	-2.28×10^{-6}	-4.54×10^{-6}	-7.77×10^{-6}
		(1.37×10^{-5})	(1.29×10^{-6})	(-5.40×10^{-6})	(-1.50×10^{-5})
		(b) $\omega = 5$ GeV			
7.61×10^{-3}	1°	1.40×10^{-7}	-2.17×10^{-7}	-4.09×10^{-7}	-6.84×10^{-7}
		(1.17×10^{-6})	(7.27×10^{-7})	(4.89×10^{-7})	(1.48×10^{-7})
1.20×10^{-1}	4°	2.72×10^{-6}	-3.11×10^{-6}	-6.24×10^{-6}	-1.07×10^{-5}
		(1.85×10^{-5})	(1.15×10^{-5})	(7.66×10^{-6})	(2.24×10^{-6})
7.03×10^{-1}	10°	2.27×10^{-5}	-1.43×10^{-5}	-3.43×10^{-5}	-6.27×10^{-5}
		(1.09×10^{-4})	(6.60×10^{-5})	(4.30×10^{-5})	(1.01×10^{-5})
3.91	30°	1.99×10^{-4}	-4.98×10^{-5}	-1.84×10^{-4}	-3.75×10^{-4}
		$(6.24 \times 10^{-4}$	(3.36×10^{-4})	(1.81×10^{-4})	(-3.97×10^{-5})
5.21	40°	3.11×10^{-4}	-3.82×10^{-5}	-2.26×10^{-4}	-4.95×10^{-4}
		(8.40×10^{-4})	(4.34×10^{-4})	(2.15×10^{-4})	(-9.80×10^{-5})
		(c) $\omega = 20$ GeV			
0.121	1°	2.69×10^{-6}	-3.04×10^{-6}	-6.13×10^{-6}	-1.05×10^{-5}
		(1.83×10^{-5})	(1.22×10^{-5})	(8.98×10^{-6})	(4.34×10^{-6})
1.85	4°	6.33×10^{-5}	-2.78×10^{-5}	-7.69×10^{-5}	-1.47×10^{-4}
		(2.80×10^{-4})	(1.85×10^{-4})	(1.34×10^{-4})	(6.09×10^{-5})
9.18	10°	3.76×10^{-4}	-1.22×10^{-4}	-3.90×10^{-4}	-7.72×10^{-4}
		(1.41×10^{-3})	(8.77×10^{-4})	(5.90×10^{-4})	(1.79×10^{-4})
27.79	30°	1.89×10^{-3}	4.46×10^{-5}	-9.49×10^{-4}	-2.37×10^{-3}
		(4.46×10^{-3})	(2.36×10^{-3})	(1.22×10^{-3})	(-3.96×10^{-4})
31.26	40°	2.36×10^{-3}	2.46×10^{-4}	-8.94×10^{-4}	-2.52×10^{-3}
		(5.04×10^{-3})	(2.61×10^{-3})	(1.31×10^{-3})	(-5.55×10^{-4})
		(d) $\omega = 150$ GeV			
6.69	1°	2.40×10^{-4}	-7.74×10^{-5}	-2.48×10^{-4}	-4.93×10^{-4}
		(1.00×10^{-3})	(6.82×10^{-4})	(5.09×10^{-4})	(2.63×10^{-4})
78.89	4°	3.28×10^{-3}	-9.45×10^{-4}	-3.22×10^{-3}	-6.47×10^{-3}
		(1.21×10^{-2})	(7.60×10^{-3})	(5.19×10^{-3})	(1.74×10^{-3})
199.35	10°	1.27×10^{-2}	-1.77×10^{-4}	-7.10×10^{-3}	-1.70×10^{-2}
		(3.18×10^{-2})	(1.73×10^{-2})	(9.46×10^{-3})	(-1.69×10^{-3})
268.85	30°	2.26×10^{-2}	4.41×10^{-3}	-5.37×10^{-3}	-1.93×10^{-2}
		$(4.33 \times 10^{-2}$	(2.25×10^{-2})	(1.14×10^{-2})	(-4.60×10^{-3})
274.07	40°	2.35×10^{-2}	4.92×10^{-3}	-5.06×10^{-3}	-1.93×10^{-2}
		(4.41×10^{-2})	(2.30×10^{-2})	(1.16×10^{-2})	(-4.73×10^{-3})

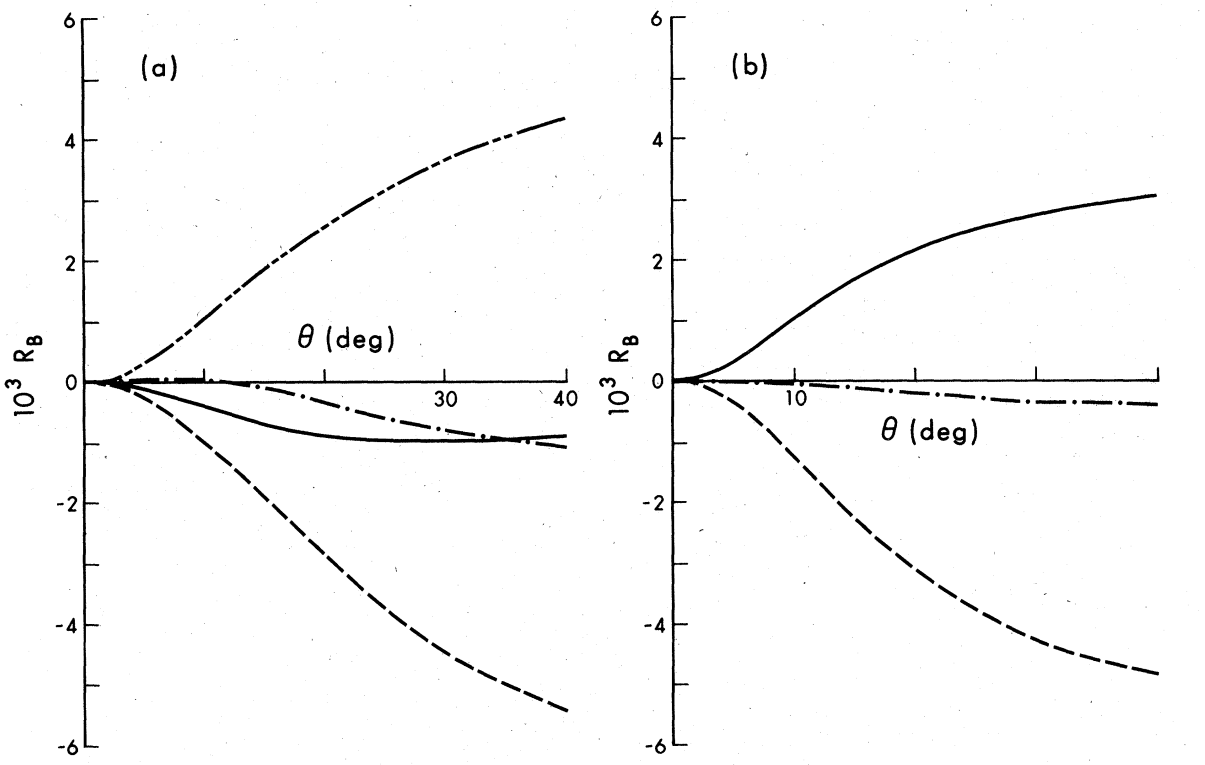

FIG. 4. The asymmetry R_B (proton target) vs scattering angle θ for different models at $\omega = 20$ GeV. (a) The standard model is given by the solid line; the $V-A$ model is given by the dashed line; the vector model ($C_V=1$, $C_A=0$) is given by the dash-dot line; and the axial-vector model ($C_A=1$, $C_V=0$) is given by the dash–double-dot line. The E_7 models with $x_W=0.4$ are given in (b), with assignment (A) given by the solid curve, (B) given by the dashed curve, and (C) given by the dot-dash curve (see Table I).

same variation with x_W is found in the neutron results of Table III, as anticipated by Eq. (22a). Again, for certain energies and values of x_W (e.g., $\omega = 20$ GeV, $x_W = 0.4$), the neutron asymmetry has a zero in the angular range considered.

A comparison of Figs. 2 and 6 reveals that the WS model predictions for polarized-beam asymmetry have the opposite sign but generally similar magnitudes to the corresponding predictions for a polarized target.

The behavior of R_T^l as a function of energy for fixed Q^2 is also similar to that of R_B. In particular, it approaches a constant at large energies. This is illustrated in Fig. 7, for the standard model.

The graphs of Fig. 8 compare the angular variation of R_T^l (proton) for the models we are considering, at a fixed energy $\omega = 20$ GeV. For larger angles, the asymmetries are very similar in all cases to the corresponding ones for a polarized beam (cf. Fig. 4), though R_T^l has the opposite sign. At small angles, the phenomenological vector model gives larger asymmetries for a polarized target than for a polarized beam, whereas for the axial-vector model, the opposite is true. This is expected from the general discussion of Sec. II [see Eqs. (15), (22a)].

The sensitivity of R_T^l (proton) to the assumed value of $M_A{}^2$ in Eq. (27g) is shown in Fig. 9. Again, the values $M_A{}^2 = 0.71$ and 1.32 GeV^2 are considered. For moderately small angles (but such that $Q^2 \gtrsim M_A{}^2$), the dependence on $M_A{}^2$ is greater than it was for a polarized beam (cf. Fig. 5) since R_T^l at small angles directly measures $C_V g_A^0$.

In Fig. 10, we show the asymmetry R_T^t for an unpolarized beam and transversely polarized proton target as a function of the scattering angle at lepton energies of 15 and 20 GeV. The polarization direction is taken to be in the scattering plane since, for polarization perpendicular to the plane, only the second-class term r_3 can contribute to the asymmetry, as discussed in Sec. II B. Once again, the standard model is assumed to obtain these results.

IV. CONCLUSIONS

We have seen that certain polarization experiments may be expected (according to several pop-

TABLE III. Values of the asymmetry R_T^I [see Eq. (20)] for the standard gauge model. (The upper number for each scattering angle θ is for a proton target and the number in parentheses is for a neutron target.)

Q^2 [(GeV/c)^2]	θ \ x_W	0.2	0.33	0.4	0.5
		(a) $\omega = 400$ MeV			
4.87×10^{-5}	1°	-1.07×10^{-9}	1.74×10^{-9}	3.26×10^{-9}	5.44×10^{-9}
		(-7.28×10^{-9})	(-2.33×10^{-9})	(3.30×10^{-10})	(4.14×10^{-9})
7.79×10^{-4}	4°	-1.75×10^{-8}	2.78×10^{-8}	5.21×10^{-8}	8.69×10^{-8}
		(-1.16×10^{-7})	(-3.73×10^{-8})	(5.34×10^{-9})	(6.63×10^{-8})
4.83×10^{-3}	10°	-1.12×10^{-7}	1.72×10^{-7}	3.25×10^{-7}	5.43×10^{-7}
		(-7.27×10^{-7})	(-2.31×10^{-7})	(3.54×10^{-8})	(4.16×10^{-7})
4.06×10^{-2}	30°	-1.21×10^{-6}	1.42×10^{-6}	2.83×10^{-6}	4.85×10^{-6}
		(-6.38×10^{-6})	(-1.93×10^{-6})	(4.63×10^{-7})	(3.88×10^{-6})
6.81×10^{-2}	40°	-2.41×10^{-6}	2.33×10^{-6}	4.88×10^{-6}	8.53×10^{-6}
		(-1.10×10^{-5})	(-3.22×10^{-6})	(9.85×10^{-7})	(7.00×10^{-6})
		(b) $\omega = 5$ GeV			
7.61×10^{-3}	1°	-1.69×10^{-7}	2.69×10^{-7}	5.04×10^{-7}	8.41×10^{-7}
		(-1.73×10^{-7})	(1.01×10^{-7})	(2.49×10^{-7})	(4.61×10^{-7})
1.20×10^{-1}	4°	-2.52×10^{-6}	3.75×10^{-6}	7.12×10^{-6}	1.19×10^{-5}
		(-2.87×10^{-6})	(1.55×10^{-6})	(3.93×10^{-6})	(7.33×10^{-6})
7.03×10^{-1}	10°	-1.39×10^{-5}	1.64×10^{-5}	3.27×10^{-5}	5.60×10^{-5}
		(-2.09×10^{-5})	(7.39×10^{-6})	(2.27×10^{-5})	(4.45×10^{-5})
3.91	30°	-1.47×10^{-4}	6.62×10^{-5}	1.81×10^{-4}	3.45×10^{-4}
		(-2.94×10^{-4})	(-5.24×10^{-5})	(7.78×10^{-5})	(2.64×10^{-4})
5.21	40°	-2.60×10^{-4}	6.11×10^{-5}	2.34×10^{-4}	4.81×10^{-4}
		(-5.17×10^{-4})	(-1.51×10^{-4})	(4.59×10^{-5})	(3.27×10^{-4})
		(c) $\omega = 20$ GeV			
0.121	1°	-2.39×10^{-6}	3.75×10^{-6}	7.06×10^{-6}	1.18×10^{-5}
		(-1.78×10^{-6})	(2.10×10^{-6})	(4.19×10^{-6})	(7.17×10^{-6})
1.85	4°	-2.47×10^{-5}	3.42×10^{-5}	6.60×10^{-5}	1.11×10^{-4}
		(-3.34×10^{-5})	(3.00×10^{-5})	(6.42×10^{-5})	(1.13×10^{-4})
9.18	10°	-1.72×10^{-4}	1.69×10^{-4}	3.53×10^{-4}	6.15×10^{-4}
		(-3.36×10^{-4})	(7.80×10^{-5})	(3.01×10^{-4})	(6.19×10^{-4})
27.79	30°	-1.67×10^{-3}	1.04×10^{-4}	1.06×10^{-3}	2.42×10^{-3}
		(-3.26×10^{-3})	(-1.23×10^{-3})	(-1.31×10^{-4})	(1.43×10^{-3})
31.26	40°	-2.21×10^{-3}	-1.31×10^{-4}	9.91×10^{-4}	2.59×10^{-3}
		(-4.23×10^{-3})	(-1.84×10^{-3})	(-5.59×10^{-4})	(1.28×10^{-3})
		(d) $\omega = 150$ GeV			
6.69	1°	-6.43×10^{-5}	9.94×10^{-5}	1.88×10^{-4}	3.13×10^{-4}
		(-9.09×10^{-5})	(1.21×10^{-4})	(2.35×10^{-4})	(3.98×10^{-4})
78.89	4°	-1.41×10^{-3}	1.44×10^{-3}	2.97×10^{-3}	5.16×10^{-3}
		(-2.90×10^{-3})	(6.91×10^{-4})	(2.62×10^{-3})	(5.38×10^{-3})
199.35	10°	-1.07×10^{-2}	1.39×10^{-3}	7.88×10^{-3}	1.72×10^{-2}
		(-2.12×10^{-2})	(-7.22×10^{-3})	(3.03×10^{-4})	(1.10×10^{-2})
268.85	30°	-2.25×10^{-2}	-4.39×10^{-3}	5.38×10^{-3}	1.93×10^{-2}
		(-4.18×10^{-2})	(-2.11×10^{-2})	(-9.91×10^{-3})	(6.04×10^{-3})
274.07	40°	-2.36×10^{-2}	-5.08×10^{-3}	4.90×10^{-3}	1.92×10^{-2}
		(-4.36×10^{-2})	(-2.24×10^{-2})	(-1.10×10^{-2})	(5.29×10^{-3})

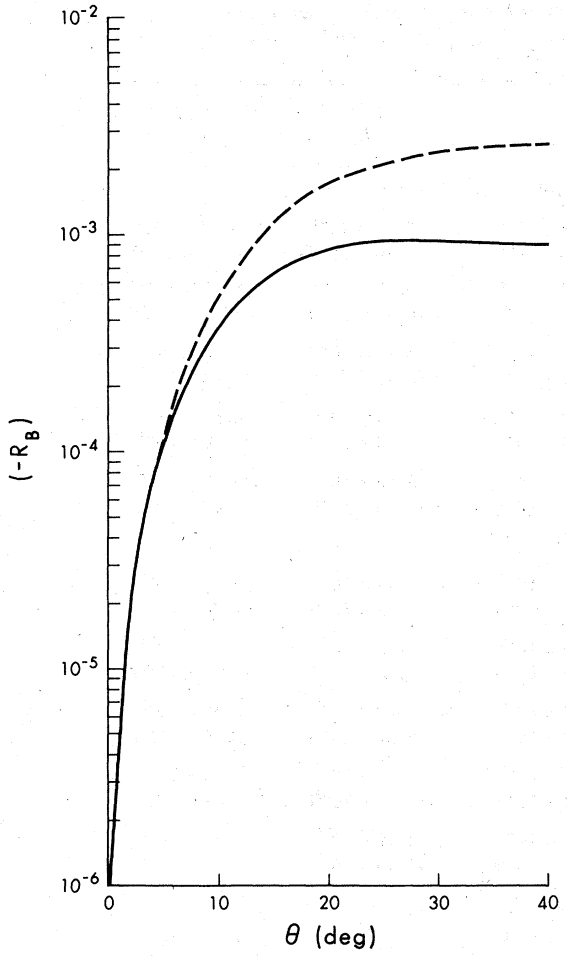

FIG. 5. R_B (proton target) vs θ at $\omega = 20$ GeV in the standard model, for the two different axial-vector masses, $M_A{}^2 = 0.71$ GeV^2 (solid curve) and $M_A{}^2 = 1.32$ GeV^2 (dashed curve).

ular theories) to produce asymmetries of 10^{-6}–10^{-5} at energies below 1 GeV, and possibly as high as several percent at energies greater than 100 GeV. [The generic equation (2), with $\mathfrak{F}$ of the order of unity, provides a useful estimate of the size of the effects.] Since the experiments presently under way at SLAC[12] may be capable of detecting asymmetries as low as 10^{-5}, there appears to be a good chance of observing these effects, and thereby gaining some knowledge of the neutral-current interactions of charged leptons.

Despite the anticipated enhancement of asymmetries at large Q^2, we have emphasized the advantages of doing experiments at Q^2 not greater than several (GeV/c)^2. One reason is theoretical; the equations (27) which were used to describe the Q^2 dependence of form factors are only approximately valid, even for small Q^2, and become increasingly unreliable as Q^2 increases. In particular, for Q^2 greater than 2–3 (GeV/c)^2, it is difficult to separate G_E and G_M for a proton, and G_E^n is even less well known.[23] All of the large-Q^2 predictions of Sec. III are subject to this basic uncertainty.

A second reason for avoiding high Q^2 is experimental. As remarked earlier, there are problems obtaining statistics, owing to rapidly falling cross sections, which can outweigh the increase in asymmetry with Q^2. To give a concrete example: in going from $\omega = 6.2$ GeV, $Q^2 = 2$ (GeV/c)^2 to $\omega = 17.3$ GeV, $Q^2 = 20$ (GeV/c)^2, the asymmetry (either R_B or R_T^l) might be expected to increase by about one order of magnitude; that is, the weak polarization effects would increase by this much relative to the basic electromagnetic rate. However, over the same kinematic range, the QED cross section, which primarily determines the measured reaction rates, falls by over four orders of magnitude.[14]

It is preferable, then, to do these polarization experiments at small Q^2. As we have discussed in Sec. II, the simplest results are obtained for $s \gg Q^2$ (in the context of Figs. 3 and 7, the asymptotic part of the curves). In this kinematic region, an experiment at only one energy and scattering angle will sometimes be sufficient to determine a particular product of leptonic and hadronic form factors [see Eqs. (15) and (22a)]. Given sufficient accuracy, such an experiment might also distinquish between several possible models of the NC, which typically have quite different predictions. However, to obtain the maximum information from a certain type of experiment, one wishes to separate all of the form factors contributing to the effect, for some given Q^2. This will require measuring the appropriate asymmetry R for fixed Q^2 and a number of values of s. This must be done in a region where R is changing with s—generally, the region where s is of the same order as Q^2 (see Figs. 3 and 7). In practice, this procedure will be very difficult, since it requires measuring small asymmetries, with good accuracy, at many energies and angles.

Even if the complete procedure described above is followed for polarized-beam experiments (the first which will likely be done), the NC will be only partly understood. Optimistically, such experiments can measure three combinations of form factors (each a product of a leptonic and hadronic form factor) and help distinguish between different models. The more difficult polarized-target experiments probe the same three form-factor combinations, but also offer the hope of testing for the second-class g_{II}^0 form factor. Two of the hadronic form factors, g_S^0 and g_P^0, can only be detected in experiments in which both beam and target are polarized.

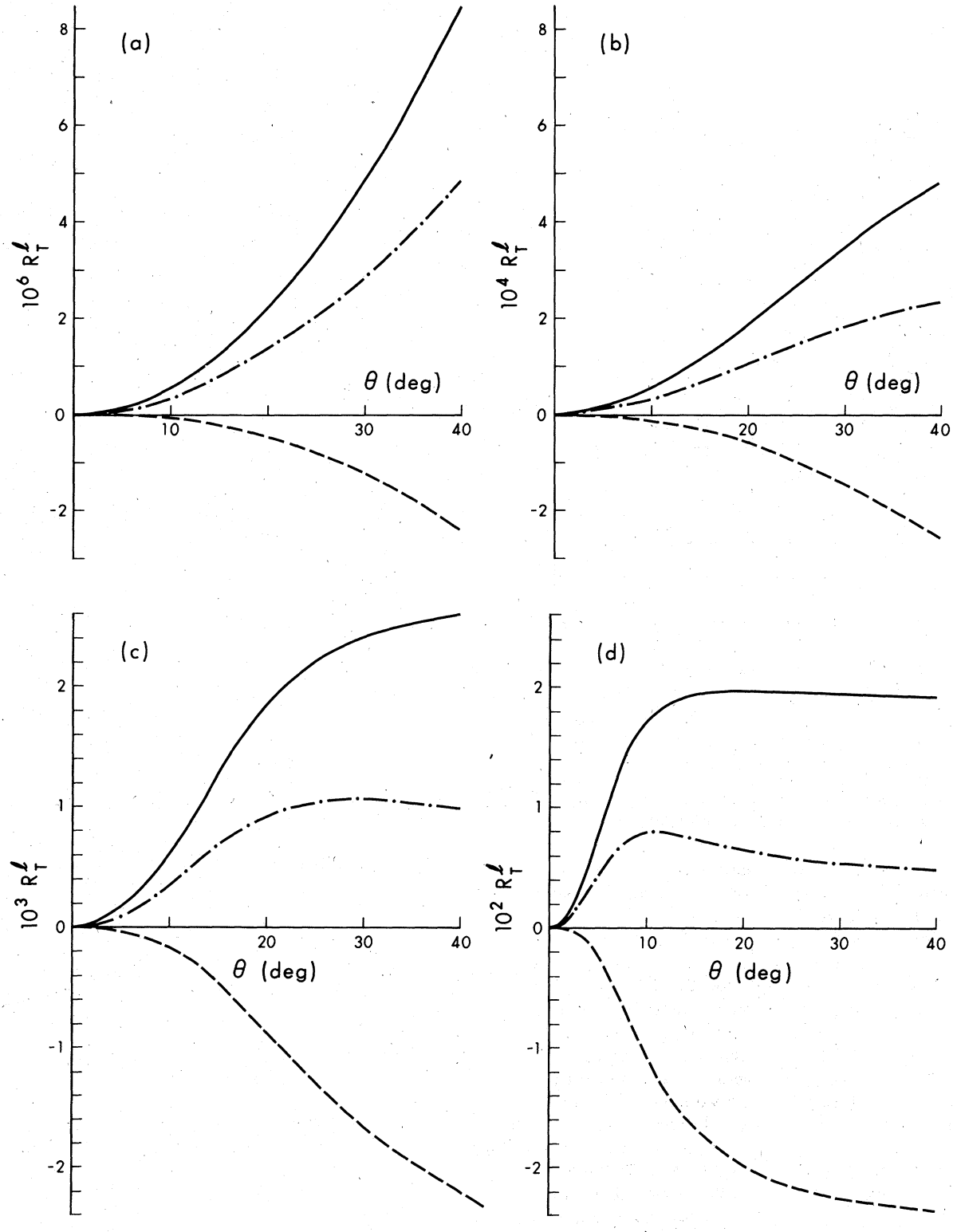

FIG. 6. The asymmetry R_T^l (see text) as a function of the scattering angle θ for a proton target and lepton energies (a) $\omega = 400$ MeV, (b) $\omega = 5$ GeV, (c) $\omega = 20$ GeV, and (d) $\omega = 150$ GeV, in the WS model. The solid curves are for $x_W = 0.5$, the dash-dot curves are for $x_W = 0.4$, and the dashed curves are for $x_W = 0.2$.

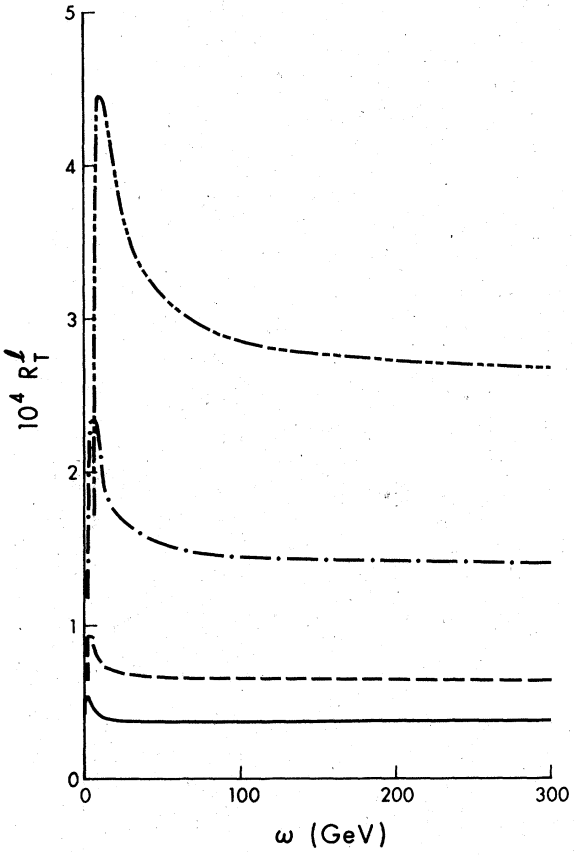

FIG. 7. The asymmetry R_T^l for a proton target as a function of incoming energy ω for different fixed Q^2 in the standard model. The solid curve is for $Q^2 = 1$ (GeV/c)^2; the dashed curve is for $Q^2 = 2$ (GeV/c)^2; the dash-dot curve is for $Q^2 = 5$ (GeV/c)^2, and the dash-double-dot curve is for $Q^2 = 10$ (GeV/c)^2.

All of these experiments must be done with both proton and deuterium targets in order to establish the isospin character of the NC.

Note added. Since the completion of this paper, we have learned of a more recent fit to the axial-vector form factor [see Eq. (27g)], using data from the Argonne-National-Laboratory–Purdue-University experiment studying the reaction $\nu_\mu + d \rightarrow \mu^- + p + p_s$. This fit gives $M_A^2 = (0.90 \pm 0.18)$ GeV^2, to be compared with our assumed values $M_A^2 = 0.71$, 1.32 GeV^2. As we have shown in Sec. III, the values of R_B are relatively insensitive to this parameter although R_T^l has slightly more dependence. Thus, the value $M_A^2 = 0.90$ GeV^2 induces a change of ~5% in the values of R_B for $\omega = 20$ GeV and $Q^2 < 5$ (GeV/c)^2 for the standard model and about 20% in the values of R_T^l for the same kinematic range.

We wish to thank Professor S. Barish for informing us of this experiment.

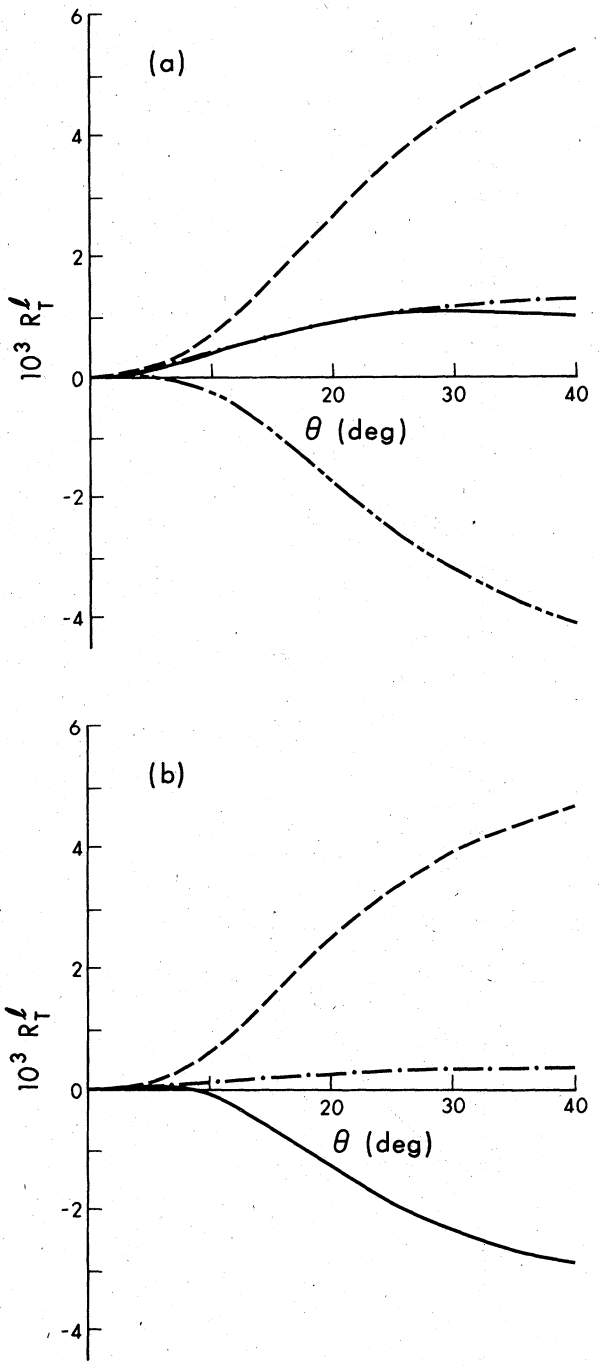

FIG. 8. The asymmetry R_T^l for a proton target vs scattering angle θ for different models at $\omega = 20$ GeV. (a) The standard model is given by the solid line, the V-A model is given by the dashed line; the vector model ($C_V = 1$, $C_A = 0$) is given by the dash-dot line; and the axial-vector model ($C_A = 1, C_V = 0$) is given by the dash-double-dot line. The E_7 models with $x_W = 0.4$ are given in (b) with assignment (A) given by the solid curve, (B) given by the dashed curve, and (C) given by the dot-dash curve (see Table I).

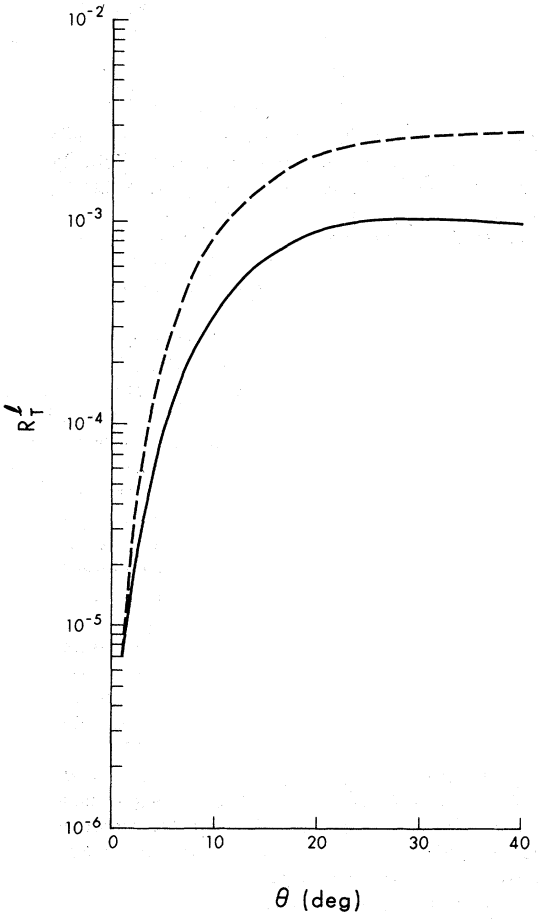

FIG. 9. R_T^l (proton target) vs θ at $\omega = 20$ GeV in the standard model, for two different axial-vector masses $M_A{}^2 = 0.71$ GeV^2 (solid curve) and $M_A{}^2 = 1.32$ GeV^2 (dashed curve).

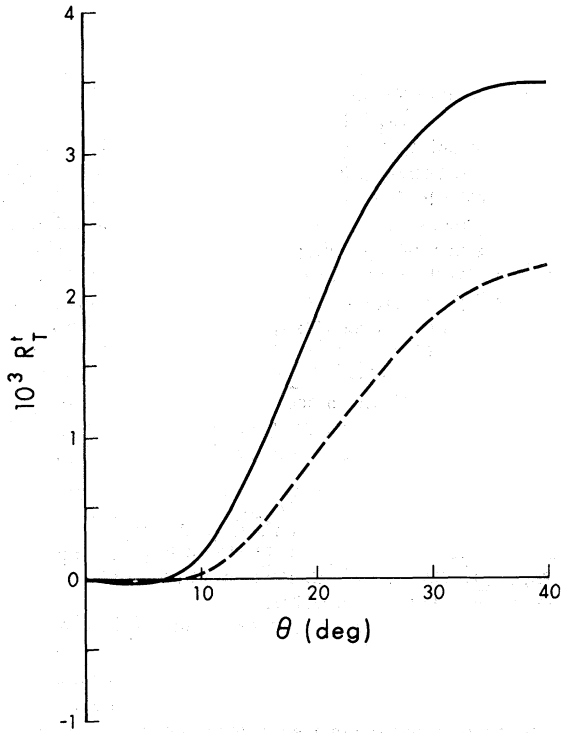

FIG. 10. The asymmetry R_T^t (see text) as a function of scattering angle θ for a proton target, in the standard model. The solid curve denotes the case $\omega = 20$ GeV and the dashed curve denotes the case $\omega = 15$ GeV.

ACKNOWLEDGMENTS

One of us (J.N.N.) would like to thank Professor S. Drell for his kind hospitality at SLAC, where this work was completed. We have enjoyed discussions with Dr. C. Prescott on the experimental aspects of the problem.

---

*Work supported in part by the National Research Council of Canada.

[1a] For measurements of $\nu_\mu N \to \nu_\mu X$, see A. Benvenuti *et al.*, Phys. Rev. Lett. 32, 800 (1974); S. J. Barish *et al.*, *ibid.* 33, 448 (1974).

[1b] For a discussion of $\nu_\mu N \to \nu_\mu N$ results, see H. H. Williams, in *Particles and Fields '76*, proceedings of the Brookhaven meeting of the Division of Particles and Fields of the American Physical Society, edited by H. Gordon and R. F. Peierls (BNL, Upton, New York, 1977), p. D95.

[1c] Results for the reaction $\nu_\mu e \to \nu_\mu e$ are given by F. J. Hasert *et al.*, Phys. Lett. 46B, 138 (1973); and, more recently, by the CERN-Gargamelle group, P. Musset, in *Proceedings of the XVIII International Conference on High Energy Physics, Tbilisi, 1976*, edited by N. N. Bogolubov *et al.* (JINR, Dubna, U. S. S. R., 1977), Vol. II, p. B87; the Aachen-Padova Collaboration, H. Faissner, *ibid.*, Vol. II, p. B114.

[2] C. H. Albright, C. Quigg, R. E. Schrock, and J. Smith, Phys. Rev. D 14, 1780 (1976); R. M. Barnett, *ibid.* 14, 2990 (1976); V. Barger and D. V. Nanopoulos, Phys. Lett. 63B, 168 (1976).

[3] The possibility of scalar and pseudoscalar NC's is deemed unlikely from analysis of the elastic neutrino-proton data of Ref. 1b. See E. Fischbach, J. T. Gruenwald, S. P. Rosen, H. Spivak and B. Kayser, Phys. Rev. D 15, 97 (1977). Regarding a tensor NC, astrophysical arguments show that it alone is too small to account for the experiments in Ref. 1. See P. G. Sutherland, J. N Ng., E. Flowers, M. Ruderman, and C. Inman, *ibid.* 13, 2700 (1976).

[4] S. Weinberg, Phys. Rev. Lett. 19, 1264 (1967); 27, 1688 (1971); A. Salam, in *Elementary Particle Theory: Relativistic Groups and Analyticity (Nobel Symposium No. 8)*, edited by N. Svartholm (Almqvist and Wiksell,

Stockholm, 1968).
[5]S. Weinberg, Phys. Rev. D 5, 1412 (1972).
[6]D. E. G. Baird *et al.*, Nature 264, 528 (1976).
[7]E. M. Henley and L. Wilets, Phys. Rev. A 14, 1411 (1976); I. Khriplovich, Zh. Eksp. Teor. Fiz. Pis'ma Red. 20, 686 (1974) [JETP Lett. 20, 315 (1974)]; M. A. Bouchiat and C. C. Bouchiat, Phys. Lett. 48B, 111 (1974); G. Feinberg and M. Y. Chen, Phys. Rev. D 10, 190 (1974); R. O. Cowan, S. Meshkov and S. P. Rosen, 1977 National Bureau of Standards report (unpublished).
[8]For a review of possible experiments, see, for example, L. Wolfenstein, in *Proceedings of the 1975 International Symposium on Lepton and Photon Interactions at High Energies, Stanford, California*, edited by W. T. Kirk (SLAC, Stanford, 1975).
[9]One exception is elastic $\nu_\mu e$ scattering. See Ref. 1c.
[10]Polarization effects in deep-inelastic eN scattering were considered by E. Derman, Phys. Rev. D 7, 2755 (1973). See also S. Berman and J. Primack, *ibid.* 9, 2171 (1974).
[11]G. Feinberg, Phys. Rev. D 12, 3575 (1975); 13, 2164 (E) (1976); S. M. Bilen'kii, N. A. Dadayan, E. Kh. Khristova, Yad. Fiz. 21, 1271 (1975) [Sov. J. Nucl. Phys. 21, 657 (1975)]; E. Reya and K. Schilcher, Phys. Rev. D 10, 952 (1974).
[12]C. Y. Prescott *et al.*, SLAC Proposal No. E-122 (unpublished).
[13]There may be more than one Z boson mediating the NC interaction. Our general formulation in Sec. II will accommodate this possibility if the coupling strength is chosen appropriately.
[14]P. N. Kirk *et al.*, Phys. Rev. D 8, 63 (1973).
[15]Our metric and γ-matrix conventions are those of J. D. Bjorken and S. D. Drell, *Relativistic Quantum Fields* (McGraw-Hill, New York, 1965).
[16]We define first-class currents as those with the same charge-conjugation properties as the corresponding quark-model currents. Second-class currents have the opposite charge-conjugation properties to the quark-model currents.
[17]R. G. Sachs, Phys. Rev. 126, 2256 (1962).
[18]C. Y. Prescott *et al.*, SLAC report (unpublished).
[19]In using the word "dominate" in this and later discussions, we are implicitly assuming that the unknown factors in the terms being compared are of similar magnitude. For example, here we assume that $C_A g_V^0$ is not too different from $C_V g_A^0$.
[20]C. Y. Prescott, personal communication.
[21]F. Gürsey and P. Sikivie, Phys. Rev. Lett. 36, 775 (1976); P. Sikivie and F. Gürsey, Phys. Rev. D 16, 816 (1977).
[22]A. De Rújula, H. Georgi, and S. L. Glashow, Phys. Rev. D 12, 3589 (1975); F. A. Wilczek, A. Zee, R. L. Kingsley, and S. B. Treiman, *ibid.* 12, 2768 (1975); H. Fritzsch, M. Gell-Mann, and P. Minkowski, Phys. Lett. 59B, 256 (1975); S. Pakvasa, W. Simmons, and S. F. Tuan, Phys. Rev. Lett. 35, 702 (1975).
[23]The proton electromagnetic form factors are discussed, for example, by Kirk *et al.*, Ref. 14, and the neutron electromagnetic form factors by K. M. Hanson *et al.*, *ibid.* 753 (1973). Further discussion of fits to these form factors may be found in W. Bartel *et al.*, Nucl. Phys. B58, 429 (1973) and references therein.
[24]The weak form factors g_V, g_T, and g_A are discussed, for example, by P. A. Schreiner, in *Neutrinos—1974*, Proceedings of the Fourth International Conference on Neutrino Physics and Astrophysics, Philadelphia, edited by C. Baltay (A.I.P., New York, 1974).
[25]The precise form of the dependence on x_W, and indeed all of the neutron predictions, are contingent upon the validity of the assumptions (27c, 27d) for the electromagnetic form factors. These assumptions must be regarded as only approximate in the light of present experimental information (see Ref. 23).